Design and Equipment Sizing of a Lab-Scale Post-Combustion CO_2 Capture Unit

Vasiliki Kontou[a], Michail Kontrafouris[a], and Sotirios Karellas[a]

[a] *Laboratory of Thermal Processes, National Technical University of Athens, Greece*
vkontou@mail.ntua.gr

Abstract:

Laboratory-scale CO_2 capture facilities are essential for validating process models and developing novel solvents for post-combustion carbon capture applications. This study details the engineering design and equipment sizing for a bench-scale chemical absorption unit capable of capturing CO_2 from gas cylinders. The system design includes absorption and desorption packed columns, cross heat exchanger, reboiler, condenser, storage tanks, and pumping systems. Column dimensions are determined using mass transfer rate equations and flooding correlations for various random packing materials including Pall rings and Raschig rings with both absorber and stripper heights fixed at 2 m. Heat exchanger sizing is performed based on LMTD method. The unit is designed to process up to 25 kg/h of flue gas containing up to 45% CO_2 using amine solvents, achieving at least 90% CO_2 capture efficiency. Detailed 3D design, equipment specifications, and control strategies are presented. The designed system provides operational flexibility for investigating absorption/desorption kinetics, solvent screening, and process parameter optimisation within a controlled laboratory environment.

Keywords:

Post-combustion carbon capture; MEA absorption; packed column design; flue gas sequestration; lab-scale CO_2 capture

1. Introduction

The continuous increase in atmospheric CO_2 concentrations in the atmosphere has driven the development and deployment of technologies and measures aimed at mitigating CO_2 emissions across emission intensive sectors. Among these technologies, carbon capture technologies play a central role for mitigating CO_2 emissions by enabling the separation of CO_2 from industrial flue gases before them being released into the atmosphere. Captured CO_2 can subsequently be permanently stored in geological formations or utilised as a feedstock for the synthesis of fuels and chemicals within Power-to-X and Carbon Capture and Utilisation (CCU) pathways contributing to both emissions reduction and resource circularity [1]. Solvent-based post-combustion CO_2 capture (PCC) through chemical absorption/stripping is currently the most mature and widely implemented technology for large-scale applications. Aqueous monoethanolamine (MEA), typically employed at 30 wt.% concentration remains the benchmark solvent due to its high reactivity with CO_2, fast reaction kinetics, low cost, extensive literature database and proven industrial maturity [2], [3], [4].

Despite its technological maturity, the primary limitation of MEA PCC systems lies in the high energy requirement for the regeneration of the solvent in the stripping column. The reboiler duty typically ranges between 2.6 to 5.0 MJ/kg of CO_2 captured for conventional MEA systems, depending on operational conditions [5], [6]. This energy penalty significantly impacts the overall efficiency of power generation systems or leads to additional utilities for other industries and remains a key barrier to large-scale deployment across various industrial settings. Consequently, reducing the regeneration energy while maintaining high capture efficiency remains a central objective in PCC research.

Laboratory and pilot scale facilities are essential for advancing PCC technologies enabling investigation of new solvents and materials and process optimisation under varying and controlled operating conditions. Laboratory and small pilot scale MEA studies use continuously operated absorber/stripper loops with column diameters ranging from 0.05–0.125 m, packing heights of 1–4.3 m in the absorber and 1-2.5 m in the stripper, and flue-gas flows of up to 100 kg/h [7], [8]. Systematic variation of flue-gas CO_2 concentration in the flue gas, solvent flow, and stripper operation parameters provides baseline design data and identifies optimal L/G ratios and

operating points for minimum regeneration energy. Lab-scale regeneration energy, typically around 4-9 MJ/kg CO_2 [7], [8].

Overall, laboratory-scale systems offer flexibility for systematic parametric studies provide experimental data for model validation. In this context, the objective of the present study is to design and analyse a modular laboratory scale PCC unit based on amine absorption/stripping. The system is intended to operate over a wide range of flue gas mass flow and composition, reflecting a wide range of industrial applications, and ensure accurate control and measurement of process variables. Emphasis is placed on flexibility and modularity. The design approach enables the adaptation of the unit to different solvents, packing materials, and operating strategies. Overall, the proposed design aims to provide a versatile experimental platform for generating reliable data, supporting process optimisation, and improving the confidence of scale-up to pilot and industrial applications.

2. Methodology

2.1. System configuration

The present study investigates the design and sizing of a modular laboratory scale PCC unit operating with aqueous amine solvents. The design basis is established using MEA operation, however, the PCC unit is designed to allow operation with various types of aqueous amines. A schematic representation of a PCC unit is shown in Figure 1. The process involves the chemical absorption of CO_2 from a flue gas at point-source. The gas mixture is introduced at the bottom of the absorption column and flow counter-current to the lean MEA solvent which is introduced at the top of the absorber and flows downward. CO_2 is absorbed from MEA through a reaction mechanism with the dominant reaction being the formation of carbamate (Eq. 1). The CO_2-rich solvent exits from the bottom of the absorber while overhead vapour is released into the atmosphere after cooling in a heat exchanger. The rich solvent is pumped to the lean/rich plate heat exchanger where it is preheated by the regenerated lean solvent and is further directed to the top of the stripper. In the stripper, the rich solvent is heated at up to 120°C resulting in the release of CO_2. Heat is supplied in most configurations as steam to the reboiler for the regeneration of the amine. Overhead vapour containing most of CO_2 is cooled in a heat exchanger and the condensates return to the top of the column while pure CO_2 exits the separation tank in gaseous phase. The regenerated lean solvent is redirected to the absorber. Before entering the absorber, the lean solvent passes through a heat exchanger to reduce its temperature to close to the absorber temperature. Liquid circulation is maintained using pumps, enabling continuous operation.

$$2MEA + CO_2 \rightleftharpoons MEACOO^- + MEAH^+ \qquad \textit{(Eq. 1)}$$

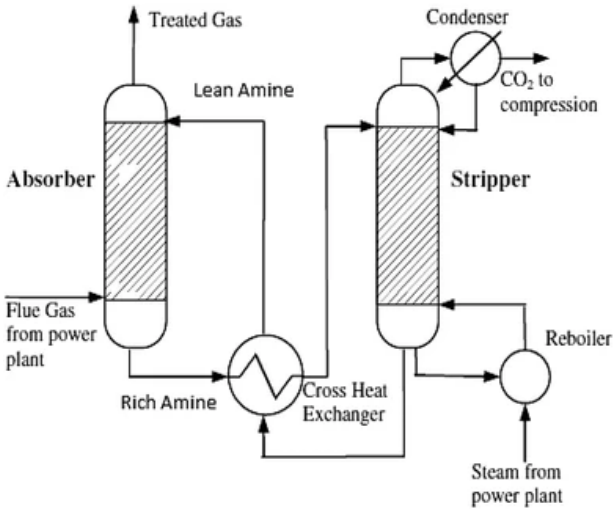

Figure 1. *Schematic of a Post Carbon Capture unit*

2.2. Design Specifications

The design and sizing of the modular PCC unit is based on laboratory-scale operational constraints and flexibility requirements. Aqueous MEA at 30 wt.% is used as the design basis solvent since it is considered a benchmark in CO_2 absorption studies [9], [10]. Higher MEA concentrations are avoided due to its viscosity and corrosivity [11]. Synthetic flue gas is supplied from compressed gas cylinders (N_2 and CO_2) and its composition, pressure and mass flow is controlled by pressure regulators and mass flow controllers. This configuration

enables the simulation of a wide range of industrial flue gas compositions (gas power production < 10%, cement ~45%) [12]. In contrast to industrial settings, the heat to the reboiler is supplied from a thermal oil due to the absence of readily available steam. Moreover, limitations regarding the space limit the total column height at 2 m. The unit is designed with a modular configuration to enable systematic variation of packing materials, solvents, materials, and operating conditions. A 90% capture efficiency is targeted which is a common design reference. Table 1 lists the main parameters adopted for the present study.

***Table 1**. Main parameters adopted for the design of the PCC unit*

Parameter	Value	Explanation
Flue gas flowrate (kg/h)	5-15	Appropriate for lab-scale
CO_2 concentration in flue gas (%)	5-45	Covers wide range and applications
Operating Pressure	1.02-2.50 bar	Typical lab conditions
Solvent	MEA	Well-established benchmark
Solvent concentration (%)	20-30	Corrosion at high concentration
Capture efficiency (%)	≥90	Industrial target
Column height (m)	≤2	Lab constraints

Thermophysical and transport properties are obtained from established correlations in the literature. Equilibrium data for CO_2 solubility in MEA at various MEA wt.% an temperatures derive from the work of Aronu et al. [13]. Thermodynamic data is determined from various sources. Viscosity of MEA is determined form Weiland at al. [14] correlations, viscosity of CO_2 loaded MEA is calculated form Amundsen et al. [15] correlations, diffusivity of CO_2 and N_2O in water derive from the work of Versteeg and van Swaaij [16], heat capacity from Weiland et al. [17], surface tension from Luo and Wand [10],vapor pressure of water from Antoine equation [18], heat of CO_2 absorption from Kim et al. [19], and equilibrium data derive from the work of Aronu et al. [13].

2.3. Column Design

In general, packed columns are selected for very corrosive materials as well as for small-scale diameters of less than 0.6 m. Therefore, packed columns are selected for the present laboratory scale configuration. The packing material influences the height and diameter of the column, and the pressure drop. Increased packing size decreases the column diameter and increases the column height. As the packing size is increased, the pressure drop per unit height of packing is reduced and the mass transfer efficiency is reduced [20], [21]. Reduced mass transfer efficiency results in a higher column. In small scale configurations, wall flow effect is observed leading to preferential flow paths (channeling and wall flow) and reduced reaction efficiency [22]. To avoid high impact of wall flow effect a minimum column diameter is selected based on the ratio of column diameter to packing size which is set at $D/d_p \geq 8$ diameter [23]. For the present configuration packing with diameter of 10 mm is used as smaller diameters are not commonly available commercially. Therefore, for the selected packing diameter, the minimum column diameter should equal $D_{min} = 80$ mm. Flooding also determines the minimum diameter of the absorber and stripper columns, and the common design is set for 60% to 80% of the flooding velocity [24]. For the present study, 60% of flooding velocity is considered to limit the system. Regarding the methodology for calculating the diameter for columns with random packings, the original Eckert flood correlation is suitable for low-capacity random packings, such as packings smaller than 1-in diameter [24].Sherwood-Leva-Eckert (SLE) generalized pressure drop correlation (GPDC) correlates the gas loading factor, the liquid loading factor, packing characteristics and pressure drop. The capacity factor CP is calculated from the equation (Eq. 2), the abscissa (flow parameter, F_{LV}) is calculated from (Eq. 3), while the operational superficial vapor velocity is considered as the 60% of flooding velocity (Eq. 4) and is used for diameter calculations (Eq. 5). The pressure drop in packed columns should not exceed 50 mmH_2O/m packing and values lower than 20 mmH_2O/m packing are preferred for absorption-stripping systems [24], [25].

$$CP = C_S F_p^{0.5} \nu^{0.05} = U_S \left(\frac{\rho_G}{\rho_L - \rho_G}\right)^{0.5} F_p^{0.5} \left(\frac{\mu_L}{g}\right)^{0.05} \quad \textit{(Eq. 2)}$$

$$F_{LV} = \frac{L}{G}\sqrt{\frac{\rho_G}{\rho_L}} \quad \textit{(Eq. 3)}$$

$$U_S = 0.60 \cdot u_{S,fl} \quad \textit{(Eq. 4)}$$

$$D = \sqrt{\frac{4G}{\pi \cdot U_S}} \quad \textit{(Eq. 5)}$$

In the above equations L and G are the liquid and gas flow rates, respectively, ρ_L and ρ_G liquid and gas densities respectively, μ_L the liquid viscosity, F_p the packing factor of the specific packing material, U_S the superficial vapor velocity, and $u_{S,fl}$ the flooding velocity.

Three different types of packing materials are investigated to assess their impact on the sizing of the unit. The packing specifications are presented in Table 2.

Table 2. *Packing specifications*

Packing Type	Size (mm)	Bulk Density (kg/m^3)	Surface Area (m^2/m^3)	Void Fraction, ε (-)	Dry Packing Factor, Fp (m^{-1})	Source
Metal Pall Rings 3/8"	10	520	515	0.94	620.05	[26]
Metal Raschig Ring 10	10	480	482	0.938	538.80	[27]
Super Raschig MSRT-01	8	230	315	0.971	343.90	[28]

For the present study, limited space availability constrains the overall height of the column, which should not exceed 2 m. The height of the column includes a packing section, a top section and a bottom section (Eq. 6). The top sections include (i) Liquid distributor, (ii) space for T and p measurements, and (iii) a wire demister and their height is limited at 0.4 m. The bottom sections include (i) gas distributor, (ii) bottom sump for liquid holdup and their height is limited at 0.4 m. Therefore, the maximum packing height is set at 1.2 m. Specifically for the stripper, to allow for space for the reboiler so that the flow from the stripper column to the kettle reboiler is primarily driven by gravity the packing height is limited to 1m.

$$H_{column} = Z_{packing} + H_{top} + H_{bot} \quad \textit{(Eq. 6)}$$

The methodology for determining the column height involves calculating the required separation, determining mass transfer coefficients, and evaluating operating and equilibrium lines. Several methods exist to determine the height of a packed column with the most widely used is the one developed from Onda et al. [29], [30]. The absorber and stripper packed heights are calculated following Onda et al. [29] methodology and involve the calculation of the effective wetted packing area, the liquid-film mass transfer coefficient, and the gas-film mass transfer coefficient. The calculation of the packed height is then calculated form the number of transfer units (NTU) based on the global driving force for the gas phase and the height of a transfer unit (HTU) based on the mass transfer correlations as seen in (Eq. 7).

$$Z_{packing} = HTU \cdot NTU \quad \textit{(Eq. 7)}$$

The NTU is calculated based on the integral of the driving force between operating and equilibrium lines based on (Eq. 8).

$$NTU = \int \frac{dy}{y - y^*} \quad \textit{(Eq. 8)}$$

The HTU is determined using mass transfer coefficients and is defined for the gas and liquid phase (Eq. 9).

$$H_{OG} = \frac{G_m}{K_y \alpha} \qquad H_{OL} = \frac{L_m}{K_x \alpha} \quad \textit{(Eq. 9)}$$

The liquid-to-gas ratio is a key design parameter affecting absorber size, capture efficiency, and regeneration duty. For a given flue gas composition and target CO_2 removal, a minimum liquid-to-gas ratio corresponds to operation approaching the equilibrium line at the rich end of the column. Under such conditions, the required packing height approaches infinity [24]. Therefore, for packed absorption systems, the liquid-to-gas ratio selected to be 1.2–2 times higher than the theoretical minimum [24].

2.4. Heat exchangers

Heat integration is incorporated in the PCC unit through a lean/rich solvent heat exchanger and two final gas coolers. The heat exchangers are sized to satisfy the thermal duties of the process under the range of operating conditions considered in the parametric analysis.

2.4.1. Lean/rich plate heat exchanger

The lean/rich plate heat exchanger is designed as a counter-current plate heat exchanger. The purpose is to recover sensible heat from the hot lean solvent exiting the stripper and transfer it to the cold rich solvent entering the stripper, thus reducing the external thermal duty of the reboiler. The plate heat exchanger is sized by the log-mean temperature difference method (LMTD) assuming counter current configuration and overall heat transfer coefficient U~400 W/m^{2}K. The heat duty of the lean/rich exchanger is obtained from the sensible heat exchanged between the rich and lean solvent streams (Eq. 10). The main equations for the sizing of the heat exchanger are presented below (Eq. 11), (Eq. 12).

$$Q = m \cdot c_p \cdot \Delta T \quad \textit{(Eq. 10)}$$

$$Q = A \cdot U \cdot \Delta T_{lm} \quad \textit{(Eq. 11)}$$

$$\Delta T_{lm} = \frac{\Delta T_1 - \Delta T_2}{\ln\left(\frac{\Delta T_1}{\Delta T_2}\right)} \quad \textit{(Eq. 12)}$$

The prediction of the rich amine exit temperature at the rich-lean plate heat exchanger derives from the correlation of Sánchez-Escalona et al. [31].

2.4.2. Lean/rich plate heat exchanger

Two water cooled shell-and-tube heat exchangers are utilized to employed to cool the exiting gas streams leaving the absorber and stripper, respectively. Each exchanger is positioned above the corresponding column. The gas stream flows through the tubes, while chilled water flows on the shell side. Cooling water is supplied from a chiller at 10^{o}C and returned at 15^{o}C. The outlet gas temperature is fixed at 20^{o}C. The thermal duty of the gas coolers is calculated from (Eq. 10) and their size is determined by (Eq. 11) and (Eq. 12).

2.4.3. Reboiler

The stripper reboiler is sized from the thermal duty required for solvent regeneration. For MEA based systems, the total reboiler duty consists of (i) the sensible heat required to raise the rich solvent temperature to the regeneration temperature, (ii) the heat of CO_2 desorption, and (iii) the heat of evaporation required to produce stripping steam (Eq. 13).

$$Q_{reb} = Q_{sens} + Q_{des,CO_2} + Q_{vap,H_2O}$$
$$Q_{reb} = \dot{m}_L c_p \left(T_{bot} - T_{top}\right) - \dot{n}_{CO_2} \Delta H_{abs,CO_2} + \dot{n}_{H_2O} \Delta H_{vap,H_2O} \quad \textit{(Eq. 13)}$$

Where m_L is the solvent mass flow rate, $\dot{n}_{CO_2}$ is the molar desorption flow rate of CO_2, $\dot{n}_{H_2O}$ is the molar flow rate of water evaporated in the reboiler, $\Delta H_{abs,CO_2}$ is the molar heat of absorption, $\Delta H_{vap,H_2O}$is the latent heat of vaporisation of water, and T_i the temperatures at the top and bottom of the stripper.

The thermal duty of the reboiler is calculated from (Eq. 10) and its size is determined by (Eq. 11) and (Eq. 12).

2.4.4. Amine system

The solvent handling system consists of a lean amine storage tank, circulation pumps, piping, and auxiliary valves for operation, drainage, solvent replacement and regulation. The total amine inventory is selected to ensure stable continuous operation over several experimental runs and to provide sufficient holdup for safe start-up, shutdown, and transient operation.

The solvent circulation system requires pumps for rich and lean amine transport between the absorber, heat exchanger, stripper, and storage tank. Pump selection is based on the required flowrate, total head, chemical compatibility with amine solutions, and controllability under low-flow laboratory conditions. Peristaltic pumps are suitable for low flowrates and corrosion resistance, whereas centrifugal pumps are more appropriate where continuous circulation and moderate head are required. The total pump head is calculated from the sum of static head, frictional pressure losses in piping and fittings, and equipment pressure drops. The pump power requirement is calculated form considering efficiency $\eta_p = 55\%$.

$$P_p = \frac{\rho g Q H_p}{\eta_p} \quad \textit{(Eq. 14)}$$

The pipe network is sized to ensure acceptable flow velocities and pressure losses. Separate criteria are applied for liquid and gas lines. Pressure drop in the pipes is calculated using the Darcy–Weisbach equation. For operation with aqueous MEA, materials should be corrosion-resistant and chemically compatible. Stainless steel and PTFE-lined components are therefore preferred.

2.5. Auxiliary

2.5.1. Gases supply

The synthetic flue gas is prepared from individual gas cylinders. For CO_2 two 50 L gas cylinders are used and for N_2 a series of nine gas cylinders is used. For gas pipelines, the design is constrained primarily by gas velocity and pressure drop. In general, velocities in gas pipelines should be limited to 20 m/s. The lower limit is defined by pressure drop. Smaller internal diameters lead to higher pressure losses, while higher diameters result in low velocities.

2.5.2. Water cooling system

A closed-loop chilled-water system is employed to remove heat from the absorber and stripper overhead gas streams and too further cool the lean amine in the amine tank. Cooling water is supplied from a recirculating chiller at 10°C and returned at 15°C ensuring outlet gas temperatures at 20°C. The distribution network is constructed using polypropylene random copolymer piping (PPR). Pipe diameters are selected to balance pressure drop and flow stability.

2.5.3. Thermal oil system

A closed-loop thermal oil circuit is employed to supply heat to the stripper reboiler, as steam is not available in the laboratory configuration. Therminol 55 thermal oil is selected for the operation. Therminol 55 is heated in an electric oil bath and circulated to the kettle reboiler, providing the required regeneration duty.

2.5.4. Instrumentation and control

The laboratory PCC unit is instrumented to ensure stable monitored operation, reproducibility of experimental conditions, and safe operation. The instrumentation includes (i) mass flow controllers (MFC) and mass flow meters (MFM), (ii) pressure gauges and pressure transmitters for column and vessel monitoring, (iii) level sensors in all vessels, (iv) temperature sensors along the columns and pipes, (v) control valves and manual isolation valves, and (vi) gas analysis instrumentation for CO_2 concentration measurement. Flow control (FIC) regulates lean solvent and gas flow rates to the absorber, rich solvent mass flow to the stripper, lean solvent mass flow to the amine tank, and thermal oil mass flow to the reboiler. Level control (LIC) protects column and flash tank flooding, and dry operation of reboiler. Temperature control (TIC) regulates reboiler temperature, the lean solvent temperature, and the gas temperature outlet. Pressure control (PIC) maintains stripper column pressure and flash drum pressure. Finally, analytical control (AIC) adjusts lean solvent flow based on CO_2 analyser reading.

3. Results

3.1. Parametric Analysis of Column Sizing and Process Performance

This chapter presents a quantitative assessment of the influence of operating conditions and design parameters on column sizing and energy performance. These results form the basis for identifying limiting design cases and selecting appropriate operating conditions for the laboratory-scale PCC unit.

The influence of flue-gas CO_2 concentration and gas flowrate on the sizing of the absorber and stripper columns was evaluated over the full design envelope. The results are presented in terms of required column diameter and packing height in Figure 2. Absorber and stripper minimum diameters increase with gas flowrate, while CO_2 concentration has an inferior effect. Higher CO_2 concentrations and higher flue gas mass flows lead to higher minimum diameters. In contrast, absorber height decreases with increasing CO_2 concentration due to enhanced mass transfer driving force, identifying dilute CO_2 (5%) as the limiting case. Stripper diameter follows similar hydrodynamic trends but shows slightly higher sensitivity to CO_2 concentration in the flue gas. Stripper height remains nearly constant (~0.45–0.55 m), indicating operation close to equilibrium. All calculated dimensions remain within the imposed design constraints (maximum column height and diameter limits), confirming that the selected configuration can accommodate the full operating envelope.

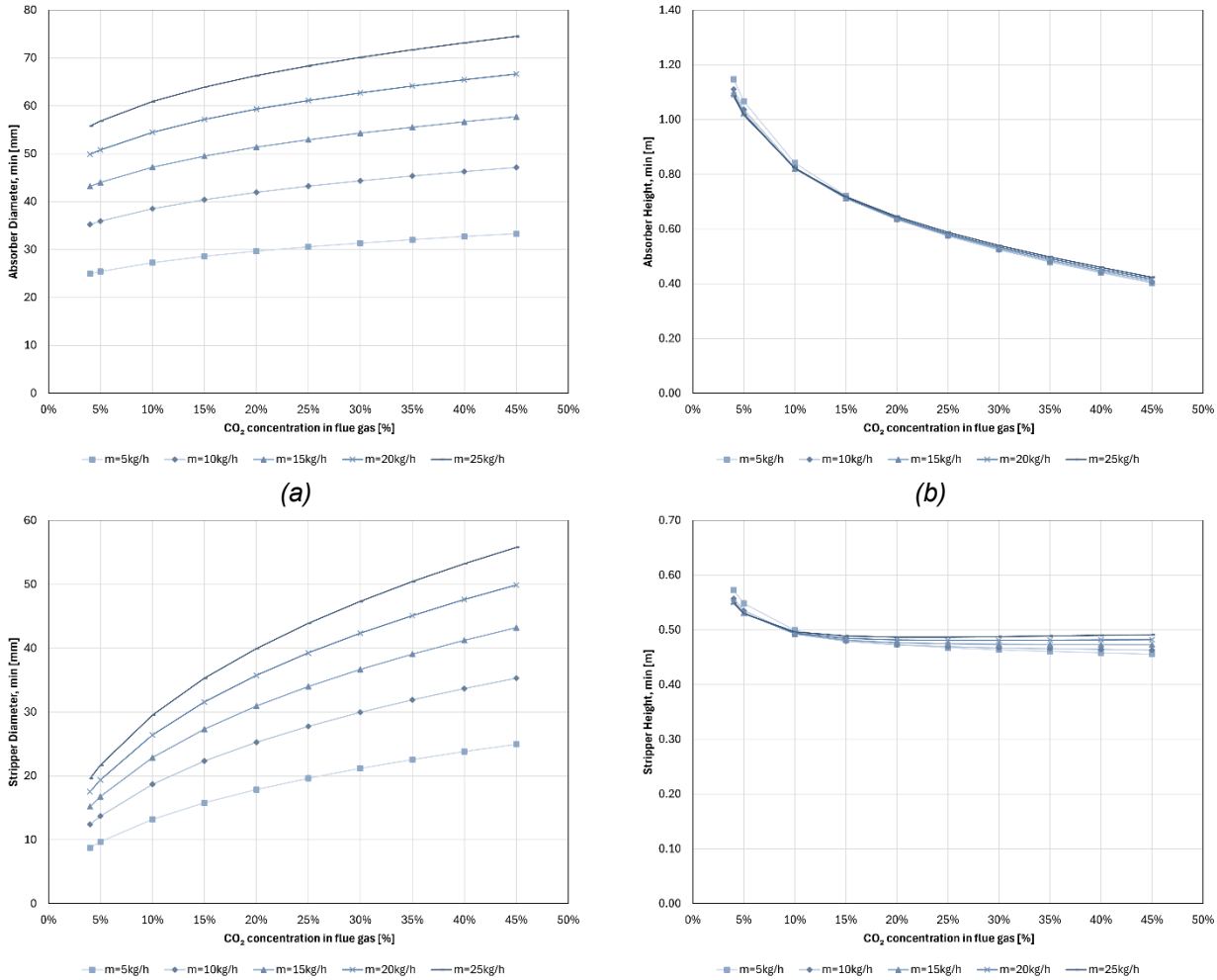

Figure 2. *Influence of flue-gas CO_2 concentration and gas flowrate column sizing: (a) absorber diameter, (b) absorber height, (c) stripper diameter, (d) stripper height or gas flowrates of 5–25 kg/h.*

The influence of packing material on column sizing was evaluated to assess its impact on column sizing across the preferred operating range. Three random packings (Metal Pall Rings 3/8”, Metal Raschig Ring 10mm, Super Raschig MSRT-01) with different characteristics, as seen in Table 2, were investigated, allowing identification of the suitability of packing materials for flexible laboratory-scale operation.

Packing material type affects both column diameter and packing height. For both absorber and stripper, Super Raschig MSRT-01 results in the lowest height by approximately two times compared to the other two types of packing material. Raschig MSRT-01 also results in the lowest diameter by approximately 15% compared to the other two types of packing material. Metal Pall Rings 3/8” and Metal Raschig Ring 10mm show comparable results. Overall, packing properties influence the design of the unit. Raschig MSRT-01packing material could accommodate larger mass flows under the spatial restrictions of the laboratory-scale unit.

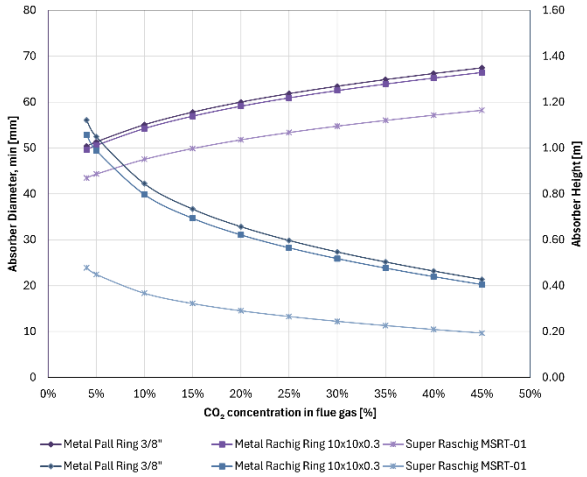

(a)

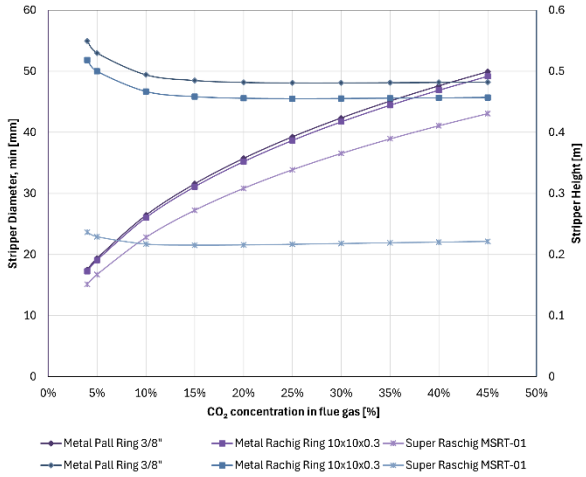

(b)

Figure 3. *Effect of packing type on absorber and stripper sizing as a function of CO_2 concentration: (a) absorber diameter and packing height, (b) stripper diameter and packing height for different random packing materials.*

The energy performance of the PCC unit was evaluated in terms of specific reboiler duty across the investigated range of flue gas CO_2 concentrations, shown in Figure 4. For each operating condition, the liquid-to-gas ratio was adjusted to ensure a constant CO_2 capture efficiency of 90%, as seen in Figure 5, allowing comparison of energy requirements under equivalent separation performance.

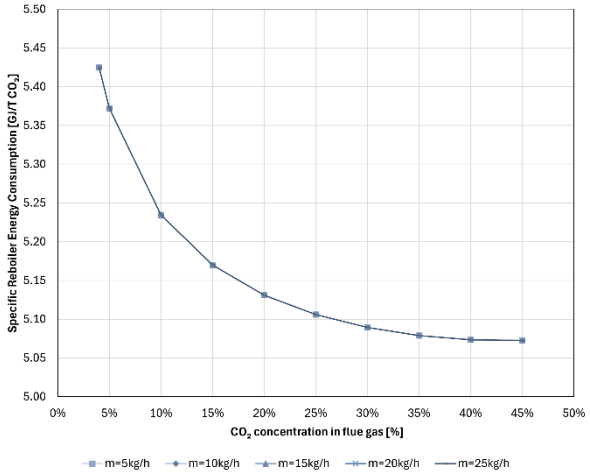

Figure 4. *Specific reboiler energy consumption as a function of flue-gas CO_2 concentration for different gas flowrates.*

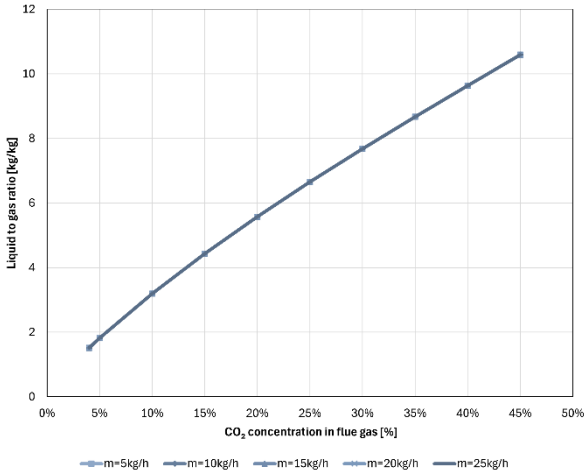

Figure 5. *Liquid-to-gas ratio on mass basis required to achieve 90% CO_2 capture as a function of flue-gas CO_2 concentration for different gas flowrates.*

The results indicate that the specific reboiler duty decreases with increasing CO_2 concentration for all investigated cases, while the required liquid-to-gas ratio increases with increasing CO_2 concentration for all operating cases to accommodate the increased CO_2 load in the gas phase while maintaining the target capture efficiency of 90%. The required liquid-to-gas ratio increases with increasing CO_2 concentration, reflecting the greater solvent circulation needed to remove the bigger CO_2 load while maintaining 90% capture. Therefore, although higher inlet CO_2 concentrations require greater solvent-to-gas ratio on a mass basis, regeneration becomes more energy-efficient per unit of CO_2 captured. The relatively high specific reboiler duty values compared to large-scale literature data are consistent with laboratory-scale operation, where thermal losses and limited heat integration are more evident.

The effect of lean solvent loading on process performance was evaluated to quantify its impact on absorber sizing and regeneration energy requirements and is presented in Figure 6. Lean loading is a key operating parameter that couples absorber and stripper performance. A lower bound of α_{lean} was identified, below which the operating line of the stripper intersects the equilibrium curve, resulting in infeasible separation. Therefore, values above this threshold are considered in the analysis. An increase in lean solvent loading results in a decrease in absorber packing height for all investigated CO_2 concentrations. The impact is more evident at low CO_2 concentrations, where the system is more sensitive to variations in solvent condition. At higher CO_2

concentrations, the dependence is less significant due to the inherently higher gas-phase driving force. In contrast, the specific reboiler duty increases with higher lean loadings. Overall, the results show the coupling between absorber performance and regeneration energy, with lean loading emerging as a key design parameter.

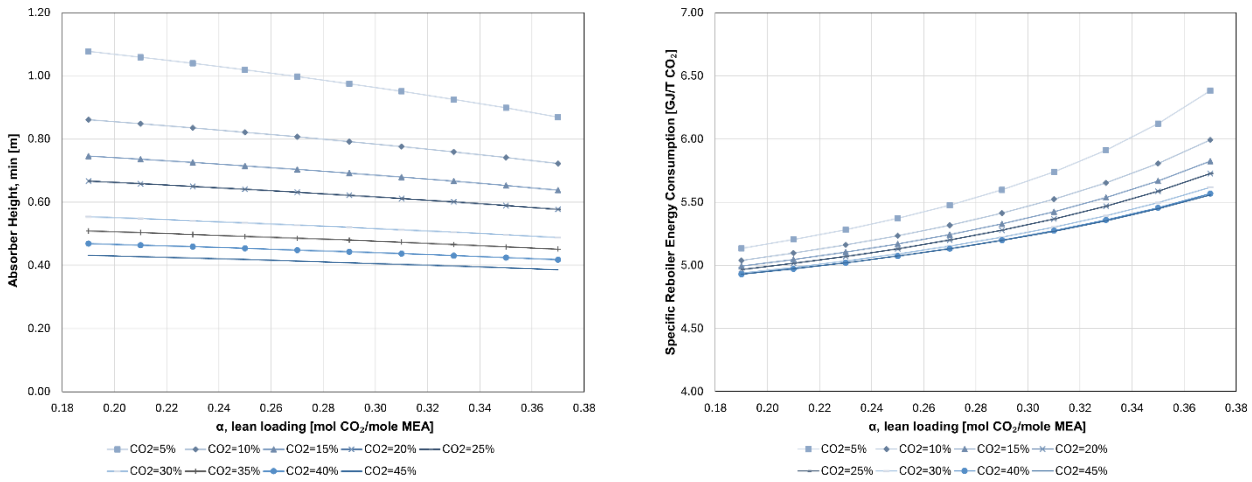

(a) *(b)*

Figure 6. *Effect of lean solvent loading on (a) absorber packing height and (b) specific reboiler duty for various CO_2 concentrations in the flue gas.*

3.2. Summary

Based on the results of the parametric analysis, a laboratory-scale PCC unit was designed to accommodate a wide range of investigated operating conditions. the selected design parameters are summarized in Table 3, The 3D design of the laboratory-scale PCC unit is presented in ***Figure 7***.

Table 3. *Design parameters for the laboratory-scale PCC unit*

Parameter	Value	
Absorber Diameter/Packing Height	0.08/1.2	m
Stripper Diameter/ Packing Height	0.08/1.0	m
Carbon Capture efficiency	90	%
Lean Loading	0.25	mol CO_2/mol MEA
Reboiler design duty	6	kW
Lean/Rich plate heat exchanger area	1	m^2
Flash tank volume	1.5	L
Pipe diameters	½”	inches
Lean/Rich pump design flowrate	3	L/min
Lean/Rich pump design head	3	m
CO_2 concentration in flues gas	5-45	%
Flue gas mass flow	5-25	kg/h
Cyclic loading	0.17-0.24	mol CO_2/mol MEA

Figure 7. *3D design of the laboratory-scale PCC unit.*

4. Conclusions

A laboratory-scale PCC unit was designed through a parametric analysis of column hydrodynamics, mass transfer performance, and energy requirements. The study provides a set of design parameters capable of operating with a wide range of flue-gas conditions while satisfying spatial and operational constraints.

Column diameter was found to be primarily restricted by gas flow rate due to hydrodynamic limitations, whereas CO_2 concentration had a secondary effect. In contrast, absorber packing height was dependent on CO_2 concentration, with the lowest concentration (5%) leading to higher column packing heights. The stripper exhibited limited sensitivity in packing height, operating close to equilibrium conditions across the examined range. Packing material selection significantly influenced column sizing. Among the evaluated options, Super Raschig MSRT-01 provided the most compact design, reducing both packing height and column diameter compared to Metal Pall Rings and Metal Raschig Ring. This highlights the importance of packing characteristics in achieving efficient and space-constrained designs at laboratory scale.

From an energy perspective, the specific reboiler duty decreased with increased CO_2 concentration, indicating improved regeneration efficiency. However, higher CO_2 concentrations required increased liquid-to-gas ratios, reflecting greater solvent circulation to maintain a constant capture efficiency of 90%. Lean solvent loading was identified as a key coupling parameter between absorber and stripper performance. Increasing lean loading reduced absorber packing requirements but resulted in higher regeneration energy demand.

Based on the parametric analysis, a representative design was selected, consisting of absorber and stripper columns with a diameter of 0.08 m, absorber packing height of 1.2 m and stripper packing height of 1m, operating at 90% CO_2 capture efficiency with a lean loading of 0.25 mol CO_2/mol amine. The reboiler duty was specified at 6 kW, and the auxiliary equipment was sized accordingly.

Nomenclature

a	CO_2 loading in solvent, mol CO_2/mol amine
A	surface area, m^2
c_p	specific heat capacity, J/(kg K)
CP	capacity parameter, -
D	diameter, m
d_p	packing diameter, mm

G gas mass flow rate, kg/s

g gravitational acceleration, m/s^2

L liquid mass flow rate, kg/s

$\dot{n}$ molar flow rate, mol/s

NTU number of transfer units

Q thermal duty, kW

T temperature, °C

U heat transfer coefficient, W/(m^2 K)

U_s superficial velocity, m/s

y gas phase mol fraction, -

Z packing height, m

Greek symbols

ε void fraction, -

η efficiency, %

ρ density, kg/m^3

μ viscosity, Pas

References

[1] S. A. Theofanidis, A. N. Antzaras, and A. A. Lemonidou, “CO2 as a building block: from capture to utilization,” *Curr. Opin. Chem. Eng.*, vol. 39, p. 100902, Mar. 2023, doi: 10.1016/j.coche.2023.100902.

[2] N. Razi, O. Bolland, and H. Svendsen, “Review of design correlations for CO2 absorption into MEA using structured packings,” *Int. J. Greenh. Gas Control*, vol. 9, pp. 193–219, Jul. 2012, doi: 10.1016/j.ijggc.2012.03.003.

[3] S. Y. W. Chai, L. H. Ngu, and B. S. How, “Review of carbon capture absorbents for CO_2 utilization,” *Greenh. Gases Sci. Technol.*, vol. 12, no. 3, pp. 394–427, Jun. 2022, doi: 10.1002/ghg.2151.

[4] S.-Y. Oh, M. Binns, H. Cho, and J.-K. Kim, “Energy minimization of MEA-based CO2 capture process,” *Appl. Energy*, vol. 169, pp. 353–362, May 2016, doi: 10.1016/j.apenergy.2016.02.046.

[5] X. Luo and M. Wang, “Improving Prediction Accuracy of a Rate-Based Model of an MEA-Based Carbon Capture Process for Large-Scale Commercial Deployment,” *Engineering*, vol. 3, no. 2, pp. 232–243, Apr. 2017, doi: 10.1016/J.ENG.2017.02.001.

[6] S. M. Soltani, P. S. Fennell, and N. Mac Dowell, “A parametric study of CO 2 capture from gas-fired power plants using monoethanolamine (MEA),” *Int. J. Greenh. Gas Control*, vol. 63, pp. 321–328, Aug. 2017, doi: 10.1016/j.ijggc.2017.06.001.

[7] A. Krótki *et al.*, “Laboratory Studies of Post-combustion CO2 Capture by Absorption with MEA and AMP Solvents,” *Arab. J. Sci. Eng.*, vol. 41, no. 2, pp. 371–379, Feb. 2016, doi: 10.1007/s13369-015-2008-z.

[8] R. Notz, H. P. Mangalapally, and H. Hasse, “Post combustion CO2 capture by reactive absorption: Pilot plant description and results of systematic studies with MEA,” *Int. J. Greenh. Gas Control*, vol. 6, pp. 84–112, 2012, doi: https://doi.org/10.1016/j.ijggc.2011.11.004.

[9] J. Kuntz and A. Aroonwilas, “Performance of Spray Column for CO_2 Capture Application,” *Ind. Eng. Chem. Res.*, vol. 47, no. 1, pp. 145–153, Jan. 2008, doi: 10.1021/ie061702l.

[10] Xiaobo Luo and Meihong Wang, “Improving Prediction Accuracy of a Rate-Based Model of an MEA-Based Carbon Capture Process for Large-Scale Commercial Deployment,” *Engineering*, vol. 3, pp. 232–243, Jan. 2017, doi: 10.1016/J.ENG.2017.02.001.

[11] E. Kayahan *et al.*, “A new look to the old solvent: Mass transfer performance and mechanism of CO2 absorption into pure monoethanolamine in a spray column,” *Chem. Eng. Process. - Process Intensif.*, vol. 184, p. 109285, Feb. 2023, doi: 10.1016/j.cep.2023.109285.

[12] L. M. Romeo, D. Catalina, P. Lisbona, Y. Lara, and A. Martínez, “Reduction of greenhouse gas emissions by integration of cement plants, power plants, and CO_2 capture systems,” *Greenh. Gases Sci. Technol.*, vol. 1, no. 1, pp. 72–82, Mar. 2011, doi: 10.1002/ghg3.5.

[13] U. E. Aronu *et al.*, “Solubility of CO2 in 15, 30, 45 and 60 mass% MEA from 40 to 120 °C and model representation using the extended UNIQUAC framework,” *Chem. Eng. Sci.*, vol. 66, no. 24, pp. 6393–6406, Dec. 2011, doi: 10.1016/j.ces.2011.08.042.

[14] R. H. Weiland, J. C. Dingman, D. B. Cronin, and G. J. Browning, “Density and Viscosity of Some Partially Carbonated Aqueous Alkanolamine Solutions and Their Blends,” *J. Chem. Eng. Data*, vol. 43, no. 3, pp. 378–382, May 1998, doi: 10.1021/je9702044.

[15] T. G. Amundsen, L. E. Øi, and D. A. Eimer, “Density and Viscosity of Monoethanolamine + Water + Carbon Dioxide from (25 to 80) °C,” *J. Chem. Eng. Data*, vol. 54, no. 11, pp. 3096–3100, Nov. 2009, doi: 10.1021/je900188m.

[16] G. F. Versteeg and W. P. Van Swaaij, “Solubility and diffusivity of acid gases (carbon dioxide, nitrous oxide) in aqueous alkanolamine solutions,” *J. Chem. Eng. Data*, vol. 33, no. 1, pp. 29–34, 1988.

[17] R. H. Weiland, J. C. Dingman, and D. B. Cronin, “Heat Capacity of Aqueous Monoethanolamine, Diethanolamine, N-Methyldiethanolamine, and N-Methyldiethanolamine-Based Blends with Carbon Dioxide,” *J. Chem. Eng. Data*, vol. 42, no. 5, pp. 1004–1006, Sep. 1997, doi: 10.1021/je960314v.

[18] P. Linstorm, “NIST chemistry webbook, NIST standard reference database number 69,” *J Phys Chem Ref Data Monogr.*, vol. 9, pp. 1–1951, 1998.

[19] I. Kim, K. A. Hoff, and T. Mejdell, “Heat of Absorption of CO2 with Aqueous Solutions of MEA: New Experimental Data,” *Energy Procedia*, vol. 63, pp. 1446–1455, 2014, doi: 10.1016/j.egypro.2014.11.154.

[20] R. P. Chhabra and M. G. Basavaraj, Eds., *Coulson and Richardson’s chemical engineering. volume 2A: particulate systems and particle technology*, Sixth edition. in Coulson & Richardson’s chemical engineering series. Oxford [England] ; Cambridge, MA: Butterworth-Heinemann, 2019.

[21] L. Valenz, J. Haidl, and V. Linek, “The Effect of Column Diameter and Packing Height on the Pressure Drop and on the HETP of Structured Packings,” *Ind. Eng. Chem. Res.*, vol. 52, no. 17, pp. 5967–5974, May 2013, doi: 10.1021/ie302397q.

[22] D. Reger, E. Merzari, S. Lee, P. Balestra, and Y. Hassan, “High-fidelity simulation of pebble beds: Toward an improved understanding of the wall channeling effect,” *ArXiv Prepr. ArXiv230805031*, 2023.

[23] R. E. Treybal, *Mass-transfer operations*, 3. ed., Reissued. in McGraw-Hill chemical engineering series. New York: McGraw-Hill, 2004.

[24] D. W. Green and M. Z. Southard, Eds., *Perry’s chemical engineers’ handbook*, Ninth edition, 85th anniversary edition. New York: McGraw Hill Education, 2019.

[25] G. Towler and R. Sinnott, *Chemical engineering design: principles, practice and economics of plant and process design*. Butterworth-Heinemann, 2021.

[26] “Metal pall ring datasheet,” MTE Group. Accessed: Apr. 20, 2026. [Online]. Available: https://www.mte-process.com/mte-process-technology/column-packing/metal-pall-ring/

[27] BOEGGER, “Cylindrical Metal Raschig Ring for Packed Columns.” Accessed: Apr. 20, 2026. [Online]. Available: https://www.randompacking.org/randompacking/metal-raschig-ring.html

[28] BOEGGER, “Metal Super Raschig Ring for Rectification Columns.” Accessed: Apr. 20, 2026. [Online]. Available: https://www.randompacking.org/randompacking/metal-super-raschig-ring.html

[29] K. Onda, E. Sada, and H. Takeuchi, “Gas absorption with chemical reaction in packed columns,” *J. Chem. Eng. Jpn.*, vol. 1, no. 1, pp. 62–66, 1968.

[30] G. Q. Wang, X. G. Yuan, and K. T. Yu, “Review of Mass-Transfer Correlations for Packed Columns,” *Ind. Eng. Chem. Res.*, vol. 44, no. 23, pp. 8715–8729, Nov. 2005, doi: 10.1021/ie050017w.

[31] A. Sánchez-Escalona, E. Góngora-Leyva, and Y. Camaraza-Medina, “Monoethanolamine Heat Exchangers Modeling Using the Buckingham Pi Theorem,” *Math. Model. Eng. Probl.*, vol. 6, no. 2, pp. 197–202, Jun. 2019, doi: 10.18280/mmep.060207.